Environmental Research Letters

LETTER • **OPEN ACCESS**

Groundwater temperature anomalies in central Europe

To cite this article: Carolin Tissen *et al* 2019 *Environ. Res. Lett.* **14** 104012

Environmental Research Letters

OPEN ACCESS

RECEIVED
1 July 2019

REVISED
4 September 2019

ACCEPTED FOR PUBLICATION
6 September 2019

PUBLISHED
15 October 2019

LETTER

Groundwater temperature anomalies in central Europe

Carolin Tissen[1], Susanne A Benz[2], Kathrin Menberg[1], Peter Bayer[3] and Philipp Blum[1]

[1] Karlsruhe Institute of Technology (KIT), Institute of Applied Geosciences (AGW), Kaiserstraße 12, Karlsruhe, Germany
[2] University of California San Diego (UCSD), School of Global Policy and Strategy (GPS), 9500 Gilman Drive, CA 92093, United States of America
[3] Ingolstadt University of Applied Sciences, Institute for new Energy Systems (InES), Esplanade 10, D-85049 Ingolstadt, Germany

E-mail: carolin.tissen@kit.edu

Keywords: anthropogenic heat intensity (AHI), CORINE land cover (CLC), groundwater temperature (GWT), temperature anomaly, central Europe

Supplementary material for this article is available online

Abstract

As groundwater is competitively used for drinking, irrigation, industrial and geothermal applications, the focus on elevated groundwater temperature (GWT) affecting the sustainable use of this resource increases. Hence, in this study GWT anomalies and their heat sources are identified. The anthropogenic heat intensity (AHI), defined as the difference between GWT at the well location and the median of surrounding rural background GWTs, is evaluated in over 10 000 wells in ten European countries. Wells within the upper three percentiles of the AHI are investigated for each of the three major land cover classes (natural, agricultural and artificial). Extreme GWTs ranging between 25 °C and 47 °C are attributed to natural hot springs. In contrast, AHIs from 3 to 10 K for both natural and agricultural surfaces are due to anthropogenic sources such as landfills, wastewater treatment plants or mining. Two-thirds of all anomalies beneath artificial surfaces have an AHI > 6 K and are related to underground car parks, heated basements and district heating systems. In some wells, the GWT exceeds current threshold values for open geothermal systems. Consequently, a holistic management of groundwater, addressing a multitude of different heat sources, is required to balance the conflict between groundwater quality for drinking and groundwater as an energy source or storage media for geothermal systems.

Abbreviations

AHI (K)	anthropogenic heat intensity
AHI_{max} (K)	upper 3% percentile of the anthropogenic heat intensity
AMD	acid mine drainage
CLC	CORINE land cover
DH	district heating
GST (°C)	ground surface temperature
GWT (°C)	groundwater temperature
GWT_r (°C)	rural background groundwater temperature
LUC	land utilisation class
r	seasonal radius
SUHI	subsurface urban heat island
URG	Upper Rhine Graben

Introduction

Groundwater is an important resource for society and industry. Within the European Union (EU), it is the main source of drinking water, supplying about 50% of the total demand [1]. However, it is equally important for agriculture. Depending on the country and type of agricultural production, up to 90% of the water for irrigation originate from groundwater [2]. In the industrial, commercial and residential sectors the use of groundwater as a resource for heating and cooling purposes is increasing worldwide [3]. Additionally, the surrounding ecosystem strongly depends on the groundwater quality and temperature [4–11]. Multiple uses of groundwater lead to high competition between different interest groups. Consequently, a holistic groundwater management in terms of quantitative, qualitative and thermal issues, as well as sensible regulations of this highly demanded source are essential [12, 13].

The EU water framework directive (WFD) [14] defines the status of groundwater in terms of quantity and chemical quality. Groundwater quality and dependent ecosystems strongly rely on physical and chemical properties, which are in turn influenced by the groundwater temperatures (GWTs) [15, 16]. The temperature determines natural bacterial and fauna community composition as well as biogeochemical processes [7, 17]. An increase in GWTs enhances the propagation of pathogen microorganisms, which in turn endanger the hygienic state of groundwater and therefore its use as a drinking water resource [8]. Thus, the WFD classifies heat input into the aquifer as pollution. However, a study by Hähnlein *et al* [18] on the legal status of shallow geothermal energy use reveals great differences between European countries: regulations are based on national or regional water management and/or ground-water protection authorities, different ministries or technical guidelines with the main purpose of the protection of groundwater as drinking water resource [19]. Furthermore, these regulations mostly concentrate on the temperature of reinjected water from industrial cooling processes and/or open geothermal systems. Until now, little attention has been paid to other anthropogenic heat sources, which may have an even larger and more widespread impact on GWTs [20–23].

Shallow GWTs are subject to seasonal variations down to a depth of 10–15 m [24]. Comparable to air temperatures, GWTs also depend on altitude and latitude [25]. For instance, mean GWT fluctuates between 2 °C and 20 °C between northern and southern Europe [26]. However, the natural state of GWT is altered by human activities. While groundwater is globally affected by increasing temperatures due to climate change [27–33], there are regional, anthropogenic impacts elevating GWT above its average and natural state. Changes in land use and advancing urbanisation in particular, directly influence groundwater recharge, level and temperature [34, 35]. Increased surface temperatures due to artificial, sealed surfaces and underground structures raise the GWT beneath cities leading to so-called subsurface urban heat islands (SUHI) [36–39]. These SUHIs are often quantified by measuring the urban heat island intensity, which is defined as the difference between GWT in the urban area and in the rural background. In Germany, Menberg *et al* [23] determined average SUHI intensities of about 3–7 K, but also detected local hot spots with GWT up to 20 K warmer than the rural background temperature.

Further GWT anomalies induced by underground car parks, construction sites, wastewater treatment plants, mine, landfills or power stations are also observed [25, 36, 40, 41]. In their study on GWTs in Germany, Benz *et al* [42] introduced the anthropogenic heat intensity (AHI), which relates average rural background temperatures to local temperature measurements. They found GWTs to be much more impacted by human activity than by atmospheric and surface temperatures. However, they did not comprehensively discuss the encountered GWT anomalies. Hence, there is still a lack of understanding of these temperature extremes, and many questions remain unanswered in regard to the locations, frequencies, implications and associated point sources of such small scale and local temperature anomalies.

This study therefore aims to map, track and discuss the occurrence of temperature anomalies in shallow aquifers in central Europe. Based on (multi-) annual mean GWT data from ten European countries (table S1 is available online at stacks.iop.org/ERL/14/104012/mmedia), we determine the corresponding anthropogenic heat intensities (AHIs) to identify extreme, positive GWT anomalies. The AHI_{max}, defined as the upper 3% percentile of all AHIs, are selected for each of the three major land cover classes (natural, agricultural and artificial) and linked to the detailed CORINE land cover types. We chose the upper 3% to assure AHIs, which are significantly above the measurement accuracy. Wells located under artificial surfaces, often in vulnerable aquifers, are examined in more detail in order to identify potential heat sources. Finally, we briefly discuss these GWT anomalies in the context of national regulations and assess the current and potential impact on our society.

Materials and methods

Groundwater temperatures

Shallow GWT data from 44 205 wells in ten countries in central Europe are the basis for this study. GWT data originate from monitoring networks and are provided by local authorities, environmental agencies or hydrogeological services (table S1). While 11% of the wells are equipped with GWT data loggers, most wells were monitored manually as part of chemical analyses. The highest well densities can be found in France, south-west Germany and Belgium, whereas only few sampled wells are located in Denmark and Slovakia (figure 1(a)). To standardise the data set and to eliminate seasonal GWT variations, data from all wells are averaged over the time span from 2003 to 2017 following the procedure given in Benz *et al* (2017a). In their approach, each temperature measurement is represented by a vector of a unit length of 1 and directed towards the month of measurement for a clocklike segmentation of the months. The output is the mean of all measurement vectors for one location,

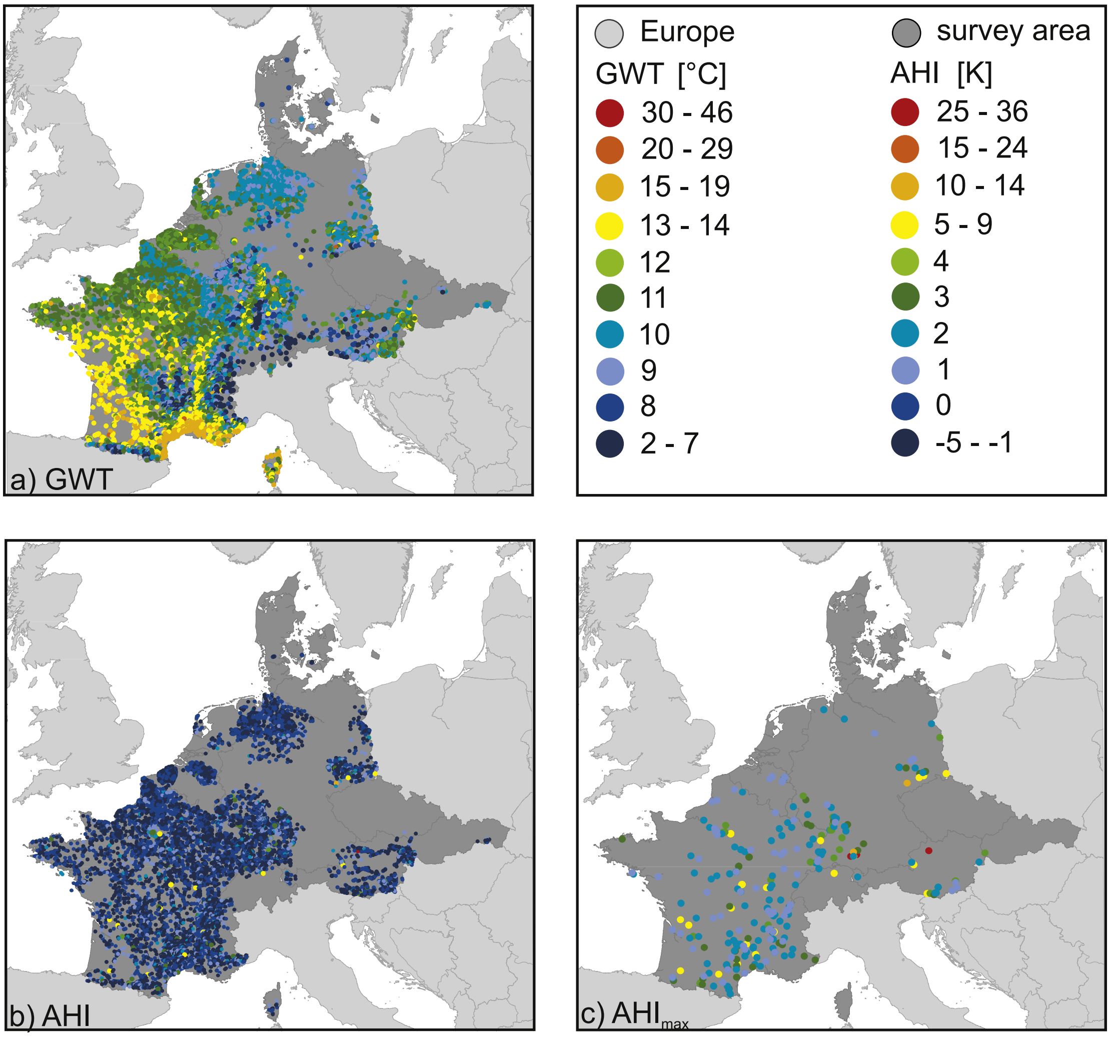

Figure 1. (a) Overview of the survey area and distribution of all 12 151 wells with bias-free annual mean groundwater temperatures (GWTs), (b) all 10 656 wells for which an anthropogenic heat intensity (AHI) could be determined, and (c) the upper 3% percentiles of the three land cover classes natural, agricultural and artificial resulting in 318 hot spots (AHI_{max}).

known as seasonal radius *r*, which is equal to zero for uniformly distributed measured data, and equal to one if they were collected in the same month. Following the recommendation by Benz *et al* (2017a), all wells with a depth $\leqslant$60 m and $r \leqslant 0.25$, which indicates a bias-free annual mean, are considered for the further analysis (figure S1).

Anthropogenic heat intensity

For each well the AHI is defined as the difference between GWT at the well location and the median of surrounding rural background GWTs (GWT_r) [42] (equation (1)). Based on the definition by Benz *et al* [42], AHI is a measure of the anthropogenic influence on GWTs. Yet, in this study AHI also detects thermal disturbances caused by natural sources, as we apply it to wells in urban as well as rural areas

$$AHI = GWT - \text{median}(GWT_r). \quad (1)$$

The input parameters to determine the rural background temperature are the bias-free GWT, geographical elevation and night-time light intensity. Elevation data are extracted from the Global 30 Arc-Second Elevation (GTOPO30) model and downloaded with Google Earth Engine [43]. Night-time lights from Version 4 of the DMSP-OLS Night-time Lights Time Series, processed by NOAA, were also extracted with Google Earth Engine. Since the night light data are only available up to January 2014, a 10 year average (01/2004 to 12/2013) was chosen. Night-time light intensity is expressed as a digital number (DN) running from 0 to 63 indicating an increasing urban activity [44]. All wells with a night-time light of $DN < 15$, an elevation $\pm$90 m and within a distance of 47 km to the analysed location are considered for the calculation of rural background temperature [42]. To ensure meaningful statistics and to avoid an impact by outliers AHI is only determined, if at least five wells fulfil these criteria.

Land cover classification

The CORINE Land Cover (CLC) [45] classification scheme consists of three hierarchical levels with 44 land cover classes at the third and most detailed level (figure S2). Based on Level 1, we define three main land cover classes: (1) natural, (2) agricultural and (3) artificial. The natural class is a combination of CLC's classes 'forest and semi natural areas' and 'wetlands'. The agricultural class contains CLC's 'agricultural areas' and the artificial class includes all 'artificial surfaces'. The calculated AHIs are categorised into and separately analysed for these three main classes (figure S3).

GWT anomalies

The wells within the upper 3% percentile of each class are specified as temperature anomalies AHI_{max}. All AHI_{max} wells within the artificial land cover class are closely inspected via satellite images (Google Earth). Based on observed common characteristics, such as land use, economic activity and settlement structures, we defined specific land utilisation classes (LUCs) with detailed subclasses and identified possible heat sources of these hot spots.

Results and discussion

Statistics of GWT anomalies (AHI_{max})

Based on the bias-free annual mean GWT (12 151 wells) an AHI could be evaluated for 10 656 wells (figure 1(b)). AHI is uniformly distributed over all known measurement depths, proving its independence of depth (figure S4). Its distribution is given in figures S5–S7. Figure 1(c) displays the wells within the top three percentiles, which represent 318 GWT anomalies (AHI_{max}) in total. 97% of these hot spots are located in Austria, France and Germany, which have the highest AHI well density overall. In Belgium, hot spots exist only in agricultural areas. Slovakia, Switzerland and Luxembourg have only one hot spot in the class artificial and natural, respectively. Czech Republic, Denmark and Netherlands do not show any (figure S8). The hot springs in Austria and Southwest Germany, as well as accumulations of hot spots in the Upper Rhine Graben (URG) and Eastern Germany clearly stand out (figure 1(c)). The URG is a densely urbanised region with multiple industrial areas, while East Germany is widely known for its former coal and ore mining. The minimum values of AHI_{max} of the classes natural, agriculture and artificial are 2.3 K, 1.7 K and 3.9 K respectively (figure S9).

To illustrate the link between land cover and temperature anomalies, the Level 3 CLC classes for wells with an AHI are compared with the CLC classes of the AHI_{max} wells (figure 2). A shift in the percentages of wells in each land cover class between these two sets is evident. Hence, it becomes apparent for which land cover temperature anomalies appear more frequently. For wells located on natural land cover, the percentage of wells in coniferous and mixed forests decreases from AHI to AHI_{max}, whereas the percentage of wells associated with transitional woodland-shrub and natural grasslands triples. The latter are therefore more likely to contain GWT anomalies. One explanation is that soil temperatures and/or GWT beneath grass or farming land are typically higher than those beneath a forest, due to differences in incident solar radiation and evapotranspiration [46, 47].

In contrast, the shift from non-irrigated arable land to pastures in the agricultural class cannot be exclusively explained by physical effects due to vegetation or shielding foliage. According to Herb *et al* [48], ground surface temperatures (GSTs) beneath grass and land with different plant canopies are similar. A possible explanation for the anomalies is deforestation, which is known to cause subsurface temperature anomalies [49–52], that are detectable at depths of 20–100 m [53]. Regarding the temporal and horizontal extent of such temperature anomalies, a lateral spread of several hundred metres over 100 years can occur [54]. Nevertheless, one has to notice that AHIs $>$ 3 K under both natural and agricultural surfaces result from hot springs or local anthropogenic sources, such as contamination caused by landfills, mining or waste water treatment plants.

In the artificial class, the share of discontinuous urban fabric shifts towards industrial areas and continuous urban fabric. Multiple previous studies on SUHIs indicated local hot spots within dense urban areas and industrial sites, which is also evident in our current findings here. Epting *et al* [41], Menberg *et al* [23] and Ferguson and Woodbury [55] noticed a strong correlation between the highest underground temperatures and the density of buildings, in particular buildings with heated basements. For the city centre of Cologne and Winnipeg, Zhu *et al* [56] found an increase in GWT of up to 5 K, which compares closely with the median of the AHI_{max} of artificial surfaces in this study (figure S9). Epting *et al* [57] observed an increase of GWT up to 6 and 8 K in dense industrial and commercial areas of Basel. Single point heat sources in industrial areas were also mentioned by Ferguson and Woodbury [58], Bucci *et al* [40] and Menberg *et al* [23].

GWT anomalies (AHI_{max}) beneath artificial surfaces

The outcome of the detailed visual inspection and examination of the surroundings of the 45 artificial AHI_{max} wells are six LUCs with 20 detailed subclasses (figures 3 and S10). With a mean AHI of 7 K, the LUC 'factory' has by far the largest impact on GWT, whereas the mean AHI of 'industry parks' is the smallest with on average 5 K. With regard to the share of each utilisation class, most of the hot spots are within 'city' (33%), followed by 'factory' and 'industry park' with 27% and 24%, respectively. In the following, possible heat sources within specific LUCs are discussed.

In the LUC 'industry park', different industrial branches such as plastic, paper, electronic, chemical or

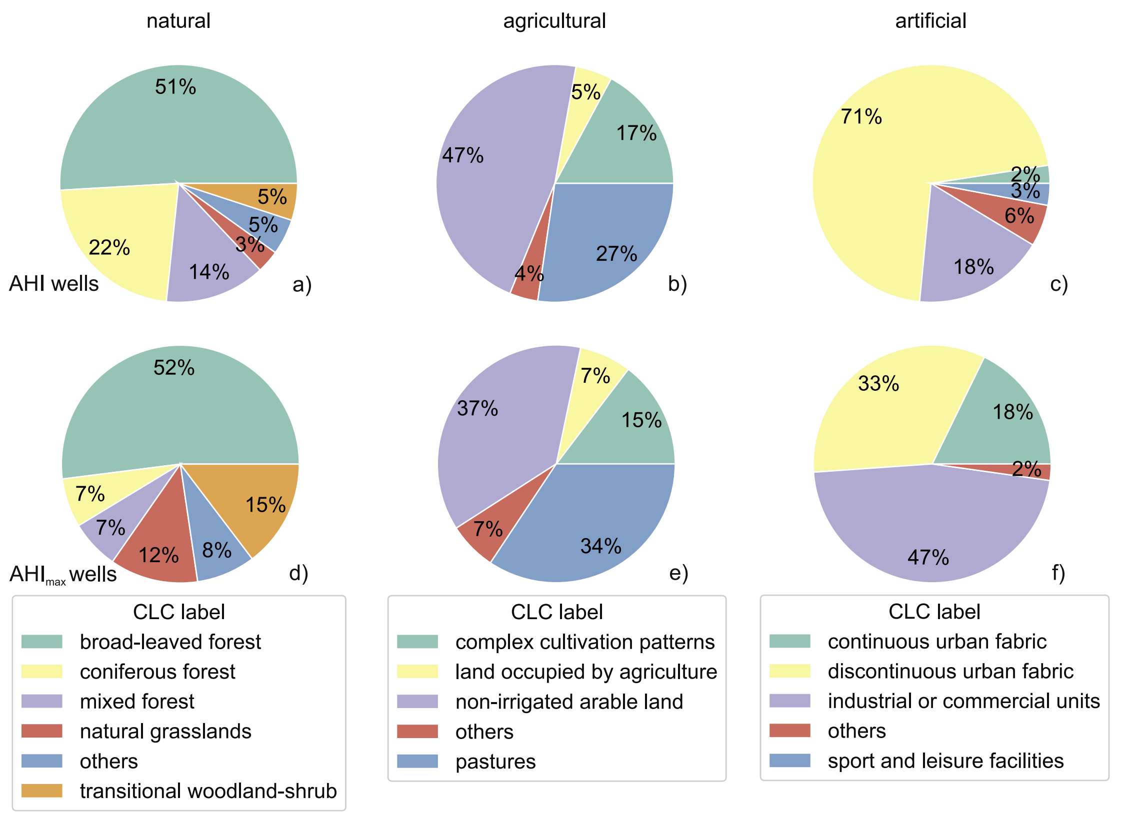

Figure 2. Percentage of wells falling into specific CORINE land cover (CLC) Level 3 classes for natural, agricultural and artificial classes, respectively. Upper row: All 10 656 wells having an anthropogenic heat intensity (AHI) (a)–(c), bottom row: 318 AHI_{max} wells representing the upper 3% percentile of all AHI wells (d)–(f).

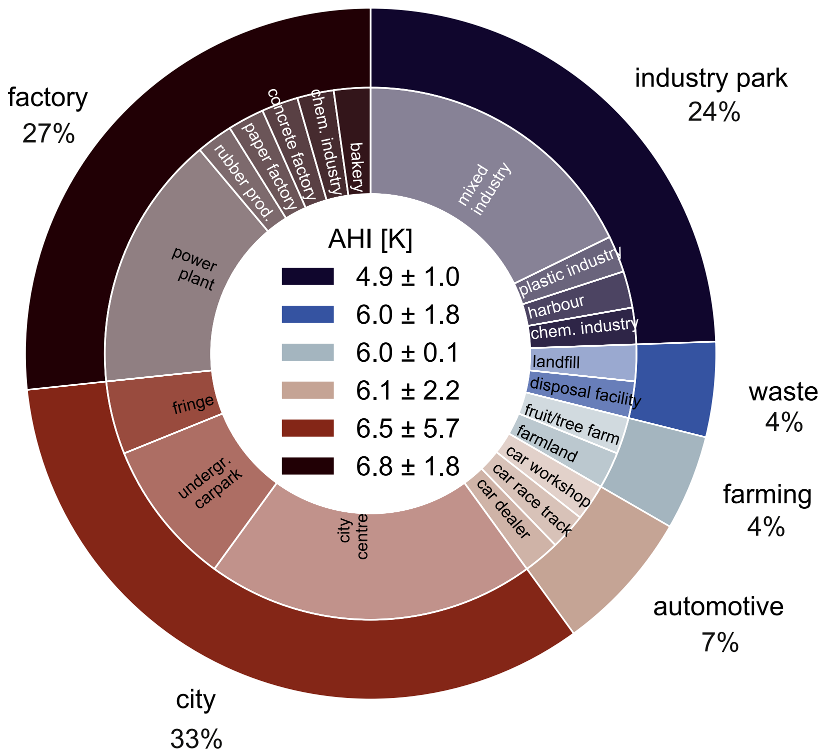

Figure 3. Segmentation of land utilisation classes (LUC, outer circle), colour coded according to their mean anthropogenic heat intensity (AHI) and standard deviation (±), and more detailed subclasses (inner circle) of the 45 AHI_{max} of artificial surfaces.

Table 1. Individual values, means and standard deviations (std) of the groundwater temperature (GWT) and anthropogenic heat intensity (AHI) for the 16 identified heat sources and seven heat source classes of the hot spots (AHI_{max}) within artificial areas.

Heat source	Nr. of locations	Parameter	Values					Mean	std
Hot spring	1	GWT (°C)	37.9					37.9	0.0
		AHI (K)	27.0					27.0	0.0
Contamination	3	GWT (°C)	23.3	18.2	17.6			19.7	2.5
		AHI (K)	9.2	7.7	4.2			7.0	2.1
Mining	2	GWT (°C)	20.9	16.7				18.8	2.1
		AHI (K)	10.6	6.2				8.4	2.2
Basement	1	GWT (°C)	15.9					15.9	0.0
		AHI (K)	4.0					4.0	0.0
District heating	3	GWT (°C)	15.6	15.4	14.3			15.1	0.6
		AHI (K)	4.4	4.2	4.0			4.2	0.1
Swimming pool	1	GWT (°C)	16.0					16.0	0.0
		AHI (K)	4.1					4.1	0.0
Undergr. car park	5	GWT (°C)	17.1	17.3	14.3	15.0	15.3	15.8	1.2
		AHI (K)	6.8	5.3	4.5	4.3	4.0	5.0	1.0

machinery construction companies are mixed with office buildings and supermarkets. Here, high GWTs can originate from multiple heat sources such as basements with heating installations, sealed surfaces or injection of cooling water. These interfere with each other and can add up so that the distinct heat source of the groundwater anomaly is difficult to identify. Bucci *et al* [40] also referred to heat fluxes from buildings into the ground originating from industrial exothermic processes inside the buildings as cause for high GWT above 17 °C in an industrial district close to Turin city.

In the LUC 'waste', one well is close to a landfill with an enclosed waste recycling plant, while the other one is on the premises of a waste disposal facility with detention basins and compensating reservoir. Benz *et al* [36] also identified a wastewater treatment plant in Osaka, Japan, as a local heat source for increased GWT.

Despite a high thematic accuracy of over 85%, wrong classifications of CLC classes can also occur [59]. Here, two wells in the artificial class are located on farmland and a fruit plantation, and thus actually fall into the agricultural class and the LUC 'farming'.

The LUC 'automotive' refers to wells located at a car workshop, a car race track and car dealer. The common characteristic of the automotive class are sealed surfaces and possible contamination with petroleum hydrocarbons [60].

The high mean AHI and standard deviation of the LUC 'city' stand out and reflect the significant, yet variable impact of the different subclasses and of the corresponding heat sources. High GWT in city centres are due to the interference and superposition of heat input by sealed surfaces and underground structures, as already described in several SUHI studies [23, 36, 38, 40, 41, 56, 61–64]. A conspicuous cluster of wells showing increased GWT were observed close to underground car parks and therefore, classified as separate subclasses. The fringe subclass contains less dense urban areas. A hot spring in Austria, having the highest AHI (27.0 K) of all artificial wells, falls within this subclass and causes the overall high AHI and standard deviation of LUC 'city'. Disregarding this natural temperature anomaly leads to a mean 'city' AHI of 5.0 ± 1.7 K.

The LUC 'factory' comprises wells situated on the property of a detached, single factory that is not part of an industrial park. All seven wells in the subclass power plant are at the same location in France, whereas the remaining subclasses are only represented by one well location each. GWT anomalies with temperatures over 30 °C in the vicinity of power plants were also reported by Menberg *et al* [23].

Heat sources of AHI_{max}

For 16 out of the 45 hot spots of the class artificial, we were able to identify potential heat sources summarised into seven classes (table 1). It is important to note that other underground heat sources such as industrial cooling, geothermal applications or sewage pipes are likely [22, 39, 40, 61], but could not be detected with the here proposed method relying on satellite imagery and local knowledge. The highest temperature anomaly is associated with a hot spring in Austria. All remaining temperature anomalies and heat source classes refer to anthropogenic activities. Based on their spatial extent and impact magnitude they can be divided into two groups. The first group consists of heat sources that are scare, but have a large extent, such as contaminations and mining operations. Basements, district heating (DH) networks, swimming pools and underground car parks are the second group. They are rather local sources, but are more frequent in urban environments and therefore also have an extensive impact on GWTs.

The first group, containing the heat sources contamination and mining, exhibits the highest GWT and AHI of all identified anthropogenic heat sources with temperatures of up to 8 K warmer than the rural surrounding. The three wells in the class contamination refer to two wells in LUC 'waste', and one well is at a car race track (LUC 'automotive'). Exothermic chemical and biological degradation processes in landfills or contaminated sites can result in higher GWTs [23, 40]. Krümpelbeck [65] reported temperatures up to 60 °C in a landfill. Similar to landfills, exothermic biogeochemical weathering processes, called acid mine drainage (AMD), cause high temperatures in mines and their remote surroundings [66]. Reports by Felix *et al* [67] and LfULG [68] confirm AMD as heat source of one particular well in the LUC subclass fringe, situated in a hard coal mining district in eastern Germany. Furthermore, they described increased GWT in remote observation wells due to coal seam fires reaching temperatures up to 90 °C within the pithead stocks. The high GWT and AHI of the well in the subclass 'farmland', located in an area in eastern Germany famous for ore mining, could also be associated with AMD.

The second group includes the small scale and local heat sources basements, DH networks, swimming pool and underground car parks. The well linked to warming from basements, is 2 m away from a shopping mall in Karlsruhe, Germany. While the AHI of this well is lower than the ones associated with contamination and mining, almost every building in a city has a basement, which typically also hosts the heating installation of the building. Epting and Huggenberger [21], Benz *et al* [61] and Epting *et al* [69] also emphasised the large impact of basements on GWT and due to their high heat flux and dominant area, named them as the dominant drivers of SUHIs.

Correlating local DH network plans with well positions, we could classify the heat source of three wells of the subclass city centre as DH. In DH networks, water with temperatures up to 160 °C circulates under high pressure through pipes under many urban areas [70]. Depending on season and type of insulation, heat losses up to 20% occur [71]. Benz *et al* [61] pointed out that DH pipes are a prominent source of anthropogenic heat fluxes. The time series in figure S11 also clearly demonstrate the impact of DH heat fluxes on a groundwater observation well 3.5 m away from the pipe. Regarding the mean GWT at 6 m depth, representing the middle of the aquifer, AHI is as high as 8 K. Consequently, the heat input by DH pipes, especially in case of a local leakage is not negligible and should be considered more carefully.

Water with lower temperatures than in DH pipes is also released into aquifers by leaking swimming pools. Cracks in the pool or loose tiles can cause leakage rates of 70 $m^3 d^{-1}$ [72]. Another case study about a municipal swimming pool in Montreal reports a leakage rate of 350–700 m^3 per day into the underlying aquifer [73]. Even if the swimming pool is watertight, the basin releases heat to the subsurface. One of the wells in LUC 'city' is located 4 m away from a municipal swimming pool in Germany and the GWT of 16 °C is likely to be influenced by the heat release of the pool. Menberg *et al* [23] even noticed a GWT of 20 °C for an observation well next to a swimming pool in Frankfurt, Germany. At another municipal swimming pool in Germany, temperatures of 25 °C beneath the swimming pool and increased GWT of 1–3 K in the downgradient were measured [74].

In previous SUHI studies, underground car parks were intensively discussed as sources for GWT anomalies [21, 22, 56]. This is in accordance with our findings that reveal underground car parks as the most frequent heat source of temperature anomalies in the class artificial (table 1). Warm, exhausted fumes and a poor ventilation lead to heat accumulation, so air temperature strongly increases in underground car parks. Iskander *et al* [75] recorded temperatures above 25 °C in summer at the lowest level of an underground car park. We also recorded air temperatures of up to 30 °C in an underground car park and correspondingly high GWT of almost 20 °C in an observation well within this car park (figure S12). The correlation between these two temperatures is obvious and therefore the heat input of underground car parks into the aquifer is evident.

Regulations

Despite the multitude of underground heat sources, only open geothermal systems are currently regulated by legally binding temperature thresholds in Austria (20 °C), Denmark (25 °C) and the Netherlands (25 °C) [76, 77]. Four wells out of all 318 hotspots exceed the 25 °C threshold value, though they are natural hot springs in Germany and Austria. A maximum temperature (T_{max}) of modified groundwater of 20 °C and a relative change (ΔT) in GWT of ±6 K is given in the geothermal installation guidelines in Austria (legally binding) and Germany (recommended) [76, 77]. For all hot spots, we detected 13 wells that exceed T_{max} and 38 with an AHI exceeding ΔT of 6 K. While four of these temperature anomalies are associated with natural hot springs, the remaining nine temperature infringements, or rather 34 for AHI exceeding ΔT, are associated with anthropogenic heat sources. The majority of wells with a higher AHI than the 6 K temperature difference (ΔT) are in the artificial land cover class and located in Austria, France, Germany and Switzerland. When comparing our results with the accepted ΔT and T_{max}, we found that the mean AHI of the LUCs 'automotive', 'city' and 'factory' are slightly above the ΔT limit, while the mean AHI linked to the heat source classes 'contamination' and 'mining' are 1 K or even more than 2 K above the criteria respectively. Since GWT is averaged, the information of seasonal positive or negative extreme values of the time series is not accounted for in this analysis. Individual GWT measurements might exceed the maximum GWT T_{max} more frequently. From the GWT time series in figures S11–S13, it becomes apparent that GWT peaks caused by basements, contamination, mining and DH surpass the

T_{max}-limit several times while annual mean values remain below the threshold. In case of aquifer thermal energy storage systems, seasonal variation of GWTs also cannot be detected by AHI since the mean GWT is equal or close to the GWT_r. Accordingly, the number of wells momentarily exceeding 20 °C is expected to be significantly higher than those found based on annual mean GWTs.

Conclusion

This study detects GWT anomalies in central Europe and identifies large- and small-scale anthropogenic heat sources such as mining and underground car parks. These extreme and until now unregulated heat sources seriously impact our groundwater. When GWTs continue to increase, groundwater cooling systems are no longer efficient [55, 69]. Furthermore, high GWT might also affect groundwater quality and ecology (e.g. [5, 6, 78–80]). In some urban areas, where aquifers are already contaminated with heavy metals and organic compounds, an increase of GWT by only 5 K might also entail a decrease of dissolved oxygen and may lead to a mobilisation of other contaminants such as arsenic [81–84]. Nevertheless, elevated GWTs provide the opportunity to harness more energy from the aquifer using shallow geothermal systems or make the operation of such systems more efficient [56, 85–88]. Overall, increased GWTs have multiple, long-term consequences and therefore, the complex interaction between heat sources and heat sinks in consideration of the aquifer characteristics should be further studied and also regulated. All these influencing factors have to be incorporated into future urban subsurface planning. Regulations should be more flexible, so that depending on the specific aims of the policy of cities and communities, the focus of groundwater management can be on groundwater as a resource for drinking water and/or as an energy resource. The use of numerical heat transport models could maximise the positive effects of increased GWT in order to meet the needs of various interest groups and to preserve the natural state of our groundwater ecosystems.

Acknowledgments

CT is grateful to the funding received through GRACE, the Graduate School for PhD students of the KIT-Center Climate and Environment at the Karlsruhe Institute of Technology (KIT). The work was also supported by the German Research Foundation (project no. B2850/3-1). The authors thank Alistair Fronhoffs (Vlaamse Milieumaatschappij), Arlette Liétar (Bruxelles Environnement), Martin Hansen (Geological Survey of Denmark and Greenland), Jürgen Gruber (Bayerisches Landesamt für Umwelt), Christian Gläser (Landesamt für Umwelt Brandenburg), Roland Funck (Der Senator für Umwelt, Bau und Verkehr), Mario Hergesell (Hessisches Landesamt für Naturschutz, Umwelt und Geologie), Lisa Beilharz (Tiefbauamt Karlsruhe), Gunter Wriedt (Niedersächsische Landesbetrieb für Wasserwirtschaft, Küsten- und Naturschutz), Peter Neumann (Landesamt für Natur, Umwelt und Verbraucherschutz), Wolfgang Plaul (Landesamt für Umwelt Rheinland-Pfalz), Sarah Melchior (Landesamt für Umwelt und Arbeitsschutz), Ulf Nilius (Landesbetrieb für Hochwasserschutz und Wasserwirtschaft Sachsen-Anhalt), Andreas Riese (Thüringer Landesamt für Umwelt und Geologie), Tom Michel (Administration de la Gestion de l'Eau), Janco van Gelderen (Informatiehuis Water), Eugen Kullman (Slovak Hydrometeorological Institute) and Jessica Stapleton (Bundesamt für Umwelt) for the provision of data and additional information. Special recognition is also given to Nicolas Weidenthaler for the field work and collection of GWT data in Mannheim, Germany. We also thank the two reviewers for their comments. We acknowledge support by the KIT-Publication Fund of the Karlsruhe Institute of Technology.

Data availability statement

The data that support the findings of this study are available from the corresponding author upon reasonable request. The data are not publicly available for legal and/or ethical reasons.

References

[1] European Commission 2016 *Synthesis Report on the Quality of Drinking Water in the Union examining Member States' Reports for the 2011–2013 Period, Foreseen Under Article 13(5) of Directive 98/83/EC* (https://eur-lex.europa.eu/legal-content/EN/TXT/?uri=CELEX%3A52016DC0666#document1)

[2] Eurostat 2019 Agri-environmental indicator—Irrigation *Stat. Explained* (https://ec.europa.eu/eurostat/statistics-explained/index.php/Agri-environmental_indicator_-_irrigation)

[3] Lund J W and Boyd T L 2016 Direct utilization of geothermal energy 2015 worldwide review *Geothermics* **60** 66–93

[4] Arning E, Kölling M, Schulz H, Panteleit B and Reichling J 2006 Einfluss oberflächennaher Wärmegewinnung auf geochemische Prozesse im Grundwasserleiter *Grundwasser* **11** 27–39

[5] Bonte M, Stuyfzand P J, van den Berg G A and Hijnen W A M 2011 Effects of aquifer thermal energy storage on groundwater quality and the consequences for drinking water production: a case study from the Netherlands *Water Sci. Technol.* **63** 1922–31

[6] Bonte M, Stuyfzand P J, Hulsmann A and Van Beelen P 2011 Underground thermal energy storage: environmental risks and policy developments in the Netherlands and European Union *Ecol. Soc.* **16** 22

[7] Brielmann H, Griebler C, Schmidt S I, Michel R and Lueders T 2009 Effects of thermal energy discharge on shallow groundwater ecosystems: ecosystem impacts of groundwater heat discharge *FEMS Microbiol. Ecol.* **68** 273–86

[8] Brielmann H, Lueders T, Schreglmann K, Ferraro F, Avramov M, Hammerl V, Blum P, Bayer P and Griebler C 2011 Oberflächennahe Geothermie und ihre potenziellen Auswirkungen auf Grundwasserökosysteme *Grundwasser* **16** 77–91

[9] Brons H J, Griffioen J, Appelo C A J and Zehnder A J B 1991 (Bio) geochemical reactions in aquifer material from a thermal energy storage site *Water Res.* **25** 729–36

[10] Griffioen J and Appelo C J 1993 Nature and extent of carbonate precipitation during aquifer thermal energy storage *Appl. Geochem.* **8** 161–76

[11] Possemiers M, Huysmans M and Batelaan O 2014 Influence of aquifer thermal energy storage on groundwater quality: a review illustrated by seven case studies from belgium *J. Hydrol.: Reg. Stud.* **2** 20–34

[12] Datta P S 2005 Groundwater ethics for its sustainability *Curr. Sci.* **89** 812–7 (http://jstor.org/stable/24111025)

[13] Flörke M, Schneider C and McDonald R I 2018 Water competition between cities and agriculture driven by climate change and urban growth *Nat. Sustain.* **1** 51–8

[14] Directive W F 2000 Directive 2000/60/EC of the European Parliament and of the Council of 23 October 2000 establishing a framework for Community action in the field of water policy *Official J. Eur. Communities* **22** 2000 (https://eur-lex.europa.eu/resource.html?uri=cellar:5c835afb-2ec6-4577-bdf8-756d3d694eeb.0004.02/DOC_1&format=PDF)

[15] Riedel T 2019 Temperature-associated changes in groundwater quality *J. Hydrol.* **572** 206–12

[16] Sharma L, Greskowiak J, Ray C, Eckert P and Prommer H 2012 Elucidating temperature effects on seasonal variations of biogeochemical turnover rates during riverbank filtration *J. Hydrol.* **428–429** 104–15

[17] Hall E K, Neuhauser C and Cotner J B 2008 Toward a mechanistic understanding of how natural bacterial communities respond to changes in temperature in aquatic ecosystems *ISME J.* **2** 471–81

[18] Hähnlein S, Molina-Giraldo N, Blum P, Bayer P and Grathwohl P 2010 Ausbreitung von Kältefahnen im Grundwasser bei Erdwärmesonden *Grundwasser* **15** 123–33

[19] Tsagarakis K P *et al* 2018 A review of the legal framework in shallow geothermal energy in selected European countries: need for guidelines *Renew. Energy* (https://doi.org/10.1016/j.renene.2018.10.007)

[20] Epting J 2017 Thermal management of urban subsurface resources–Delineation of boundary conditions *Proc. Eng.* **209** 83–91

[21] Epting J and Huggenberger P 2013 Unraveling the heat island effect observed in urban groundwater bodies-definition of a potential natural state *J. Hydrol.* **501** 193–204

[22] Menberg K, Blum P, Schaffitel A and Bayer P 2013 long-term evolution of anthropogenic heat fluxes into a subsurface urban heat island *Environ. Sci. Technol.* **47** 9747–55

[23] Menberg K, Bayer P, Zosseder K, Rumohr S and Blum P 2013 Subsurface urban heat islands in German cities *Sci. Total Environ.* **442** 123–33

[24] Taylor C A and Stefan H G 2009 Shallow groundwater temperature response to climate change and urbanization *J. Hydrol.* **375** 601–12

[25] Benz S A, Bayer P and Blum P 2017 Global patterns of shallow groundwater temperatures *Environ. Res. Lett.* **12** 034005

[26] Bonsor H C 2017 *Groundwater, geothermal modelling and monitoring at city-scale: reviewing European practice and knowledge exchange: TU1206 COST sub-urban WG2 report* British Geological Survey

[27] Beltrami H, Ferguson G and Harris R N 2005 Long-term tracking of climate change by underground temperatures *Geophys. Res. Lett.* **32**

[28] Benz S A, Bayer P, Winkler G and Blum P 2018 Recent trends of groundwater temperatures in Austria *Hydrol. Earth Syst. Sci.* **22** 3143–54

[29] Green T R, Taniguchi M, Kooi H, Gurdak J J, Allen D M, Hiscock K M, Treidel H and Aureli A 2011 Beneath the surface of global change: impacts of climate change on groundwater *J. Hydrol.* **405** 532–60

[30] Gunawardhana L N and Kazama S 2012 Statistical and numerical analyses of the influence of climate variability on aquifer water levels and groundwater temperatures: the impacts of climate change on aquifer thermal regimes *Glob. Planet. Change* **86–87** 66–78

[31] Kurylyk B L, Bourque C P-A and MacQuarrie K T B 2013 Potential surface temperature and shallow groundwater temperature response to climate change: an example from a small forested catchment in east-central New Brunswick (Canada) *Hydrol. Earth Syst. Sci.* **17** 2701–16

[32] Menberg K, Blum P, Kurylyk B L and Bayer P 2014 Observed groundwater temperature response to recent climate change *Hydrol. Earth Syst. Sci.* **18** 4453–66

[33] Singh R D and Kumar C P 2010 Impact of climate change on groundwater resources *Int. J. Clim. Change Strateg. Manage.* **1** 15

[34] Colombani N, Giambastiani B M S and Mastrocicco M 2016 Use of shallow groundwater temperature profiles to infer climate and land use change: interpretation and measurement challenges: effect of land use and climate changes on groundwater temperature *Hydrol. Process.* **30** 2512–24

[35] Sharp J M 2010 The impacts of urbanization on groundwater systems and recharge *AQUA mundi* **1** 51–6

[36] Benz S A, Bayer P, Blum P, Hamamoto H, Arimoto H and Taniguchi M 2018 Comparing anthropogenic heat input and heat accumulation in the subsurface of Osaka, Japan *Sci. Total Environ.* **643** 1127–36

[37] Ferguson G and Woodbury A D 2007 Urban heat island in the subsurface *Geophys. Res. Lett.* **34** L23713

[38] Taniguchi M, Uemura T and Jago-on K 2007 Combined effects of urbanization and global warming on subsurface temperature in four asian cities *Vadose Zone J.* **6** 591

[39] Zhu K, Bayer P, Grathwohl P and Blum P 2015 Groundwater temperature evolution in the subsurface urban heat island of Cologne, Germany *Hydrol. Process.* **29** 965–78

[40] Bucci A, Barbero D, Lasagna M, Forno M G and De Luca D A 2017 Shallow groundwater temperature in the Turin area (NW Italy): vertical distribution and anthropogenic effects *Environ. Earth Sci.* **76**

[41] Epting J, Scheidler S, Affolter A, Borer P, Mueller M H, Egli L, García-Gil A and Huggenberger P 2017 The thermal impact of subsurface building structures on urban groundwater resources—a paradigmatic example *Sci. Total Environ.* **596–597** 87–96

[42] Benz S A, Bayer P and Blum P 2017 Identifying anthropogenic anomalies in air, surface and groundwater temperatures in Germany *Sci. Total Environ.* **584–585** 145–53

[43] Engine G E 2015 Google earth engine: a planetary-scale geospatial analysis platform (https://earthengine.google.com)

[44] Li D, Zhao X and Li X 2016 Remote sensing of human beings—a perspective from night-time light *Geo-Spat. Inf. Sci.* **19** 69–79

[45] CORINE, CORINE Land Cover-Copernicus Land Monitoring Service. 2016; (https://land.copernicus.eu/pan-european/corine-land-cover)

[46] Beltrami H and Kellman L 2003 An examination of short- and long-term air-ground temperature coupling *Glob. Planet. Change* **38** 291–303

[47] Kupfersberger H, Rock G and Draxler J C 2017 Inferring near surface soil temperature time series from different land uses to quantify the variation of heat fluxes into a shallow aquifer in Austria *J. Hydrol.* **552** 564–77

[48] Herb W R, Janke B, Mohseni O and Stefan H G 2008 Ground surface temperature simulation for different land covers *J. Hydrol.* **356** 327–43

[49] van den Brink C, Frapporti G, Griffioen J and Zaadnoordijk W J 2007 Statistical analysis of anthropogenic versus geochemical-controlled differences in groundwater composition in The Netherlands *J. Hydrol.* **336** 470–80

[50] Foley J A 2005 Global consequences of land use *Science* **309** 570–4

[51] Lewis T J and Wang K 1998 Geothermal evidence for deforestation induced warming: implications for the Climatic impact of land development *Geophys. Res. Lett.* **25** 535–8

[52] Taniguchi M, Williamson D R and Peck A J 1999 Disturbances of temperature-depth profiles due to surface climate change and subsurface water flow: II. An effect of step increase in

surface temperature caused by forest clearing in southwest western Australia *Water Resour. Res.* **35** 1519–29

[53] Ferguson G and Beltrami H 2006 Transient lateral heat flow due to land-use changes *Earth Planet. Sci. Lett.* **242** 217–22

[54] Bense V and Beltrami H 2007 Impact of horizontal groundwater flow and localized deforestation on the development of shallow temperature anomalies *J. Geophys. Res.* **112**

[55] Ferguson G and Woodbury A D 2004 Subsurface heat flow in an urban environment *J. Geophys. Res.: Solid Earth* **109** B02402

[56] Zhu K, Blum P, Ferguson G, Balke K-D and Bayer P 2010 The geothermal potential of urban heat islands *Environ. Res. Lett.* **5**

[57] Epting J, García-Gil A, Huggenberger P, Vázquez-Suñe E and Mueller M H 2017 Development of concepts for the management of thermal resources in urban areas–assessment of transferability from the Basel (Switzerland) and Zaragoza (Spain) case studies *J. Hydrol.* **548** 697–715

[58] Ferguson G and Woodbury A D 2005 Thermal sustainability of groundwater-source cooling in Winnipeg, Manitoba *Can. Geotech. J.* **42** 1290–301

[59] EEA 2006 The thematic accuracy of Corine land cover 2000: assessment using LUCAS (land use cover area frame statistical survey) *Technical Report* No 7, OCLC: 836343078 EEA: Copenhagen

[60] Akankpo O and Igboekwe M U 2011 Monitoring groundwater contamination using surface electrical resistivity and geochemical methods *J. Water Resour. Prot.* **03** 318–24

[61] Benz S A, Bayer P, Menberg K, Jung S and Blum P 2015 Spatial resolution of anthropogenic heat fluxes into urban aquifers *Sci. Total Environ.* **524–525** 427–39

[62] Benz S A, Bayer P, Goettsche F M, Olesen F S and Blum P 2016 Linking surface urban heat islands with groundwater temperatures *Environ. Sci. Technol.* **50** 70–8

[63] Oke T R 1973 City size and the urban heat island *Atmos. Environ.* **7** 769–79

[64] Taniguchi M, Shimada J, Tanaka T, Kayane I, Sakura Y, Shimano Y, Dapaah-Siakwan S and Kawashima S 1999 Disturbances of temperature-depth profiles due to surface climate change and subsurface water flow: I. An effect of linear increase in surface temperature caused by global warming and urbanization in the Tokyo Metropolitan Area, Japan *Water Resour. Res.* **35** 1507–17

[65] Krümpelbeck I 2000 Untersuchungen zum langfristigen Verhalten von Siedlungsabfalldeponien *PhD Thesis* Bergischen Universität—Gesamthochschule Wuppertal, Wuppertal

[66] Willscher S, Hertwig T, Frenzel M, Felix M and Starke S 2010 Results of remediation of hard coal overburden and tailing dumps after a few decades: insights and conclusions *Hydrometallurgy* **104** 506–17

[67] Felix M, Sohr A, Riedel P and Assmann L 2009 Gefährdungspotenzial Steinkohlenhalden Zwickau/Oelsnitz —Kurzbericht zu den Forschungsberichten 2005 bis 2007 zur Thematik p 95 (https://umwelt.sachsen.de/umwelt/download/luft/42_Kurzbericht_SteinkohlenHalden_SN.pdf)

[68] LfULG 2010 Geologie und Bergbaufolgen im Steinkohlerevier Lugau/Oelsnitz—Geoprofil 13 (https://publikationen.sachsen.de/bdb/artikel/12197/documents/12905)

[69] Epting J, Händel F and Huggenberger P 2013 Thermal management of an unconsolidated shallow urban groundwater body *Hydrol. Earth Syst. Sci.* **17** 1851–69

[70] Energie W 2013 Technische Richtlinien—Technische Auslegungsbedingungen (https://wienenergie.at/media/files/2015/technische)

[71] Recknagel H, Sprenger E and Schramek E-R 2007 *Taschenbuch für Heizung+Klimatechnik 07/08* vol 73 73rd edn (München: Oldenbourg Industrieverlag)

[72] Water S 2011 Best practice guidelines for water management in aquatic leisure centre (https://sydneywater.com.au/web/groups/publicwebcontent/documents/document/zgrf/mdq1/~edisp/dd_045262.pdf)

[73] Chapuis R P 2010 Using a leaky swimming pool for a huge falling-head permeability test *Eng. Geol.* **114** 65–70

[74] Blum P 2018 Geospeicher.bw p 28 (http://fachdokumente.lubw.baden-wuerttemberg.de/servlet/is/127777/l7516014_16019_%2012.03.2019.pdf?command=downloadContent&filename=l7516014_16019_%2012.03.2019.pdf&FIS=203)

[75] Iskander M, Aboumoussa W and Gouvin P 2001 Instrumentation and monitoring of a distressed multistory underground parking garage *J. Perform. Constr. Facil* **15** 115–23

[76] Hähnlein S, Bayer P and Blum P 2010 International legal status of the use of shallow geothermal energy *Renew. Sustain. Energy Rev.* **14** 2611–25

[77] Hähnlein S, Blum P and Bayer P 2011 Oberflächennahe geothermie—aktuelle rechtliche situation in deutschland *Grundwasser* **16** 69–75

[78] Danielopol D L, Gibert J, Griebler C, Gunatilaka A, Hahn H J, Messana G, Notenboom J and Sket B 2004 Incorporating ecological perspectives in European groundwater management policy *Environ. Conserv.* **31** 185–9

[79] Hahn H J, Schweer C and Griebler C 2018 Are groundwater ecosystems rights being preserved? *Grundwasser* **23**

[80] Hähnlein S, Bayer P, Ferguson G and Blum P 2013 Sustainability and policy for the thermal use of shallow geothermal energy *Energy Policy* **59** 914–25

[81] Bonte M, Röling W F M, Zaura E, van der Wielen P W J J, Stuyfzand P J and van Breukelen B M 2013 Impacts of shallow geothermal energy production on redox processes and microbial communities *Environ. Sci. Technol.* **47** 14476–84

[82] Bonte M, van Breukelen B M and Stuyfzand P J 2013 Temperature-induced impacts on groundwater quality and arsenic mobility in anoxic aquifer sediments used for both drinking water and shallow geothermal energy production *Water Res.* **47** 5088–100

[83] Bonte M, Stuyfzand P J and Breukelen B M V 2014 Reactive transport modeling of thermal column experiments to investigate the impacts of aquifer thermal energy storage on groundwater quality *Environ. Sci. Technol.* **48** 12099–107

[84] Griebler C, Kellermann C, Kuntz D, Walker-Hertkorn S, Stumpp C and Hegler F 2014 Auswirkungen Thermischer Veränderungen Infolge der Nutzung OberfläChennaher Geothermie auf die Beschaffenheit des Grundwassers und Seiner Lebensgemeinschaften—Empfehlungen für eine umweltverträgliche Nutzung Umweltbundesamt pp 1–53 (http://bmub.bund.de/fileadmin/Daten_BMU/Pools/Forschungsdatenbank/fkz_3710_23_204_thermische_veraenderungen_bf.pdf)

[85] Arola T and Korkka-Niemi K 2014 The effect of urban heat islands on geothermal potential: examples from Quaternary aquifers in Finland *Hydrol. J.* **22** 1953–67

[86] Bayer P, Attard G, Blum P and Menberg K 2019 The geothermal potential of cities *Renew. Sustain. Energy Rev.* **106** 17–30

[87] Menberg K, Blum P, Rivera J, Benz S and Bayer P 2015 Exploring the Geothermal Potential of Waste Heat Beneath Cities *Proc. World Geothermal Congress* pp 1–5

[88] Rivera J A, Blum P and Bayer P 2017 Increased ground temperatures in urban areas: estimation of the technical geothermal potential *Renew. Energy* **103** 388–400